

## Rutherford simple and multiple scattering by computer simulation

This content has been downloaded from IOPscience. Please scroll down to see the full text.

2001 Eur. J. Phys. 22 157

(<http://iopscience.iop.org/0143-0807/22/2/308>)

View [the table of contents for this issue](#), or go to the [journal homepage](#) for more

Download details:

IP Address: 158.49.247.81

This content was downloaded on 13/03/2017 at 10:39

Please note that [terms and conditions apply](#).

You may also be interested in:

[Screened Coulomb scattering versus Thomson scattering](#)

Pascal Monceau, Thomas Szydlo and Galliano Valent

[Measuring solar limb-darkening with modest equipment](#)

F Sánchez-Bajo, J M Vaquero and M P Rubio Montero

[Large and small deflections of a cantilever beam](#)

Tarsicio Beléndez, Cristian Neipp and Augusto Beléndez

[Systematic errors in angular correlation measurements of the 3 1P state of helium](#)

Ian Humphrey

[APREFIS 1.0: a computer program for learning physics](#)

L García-Rodríguez, C González-Silgo, C Ruiz-Pérez et al.

[Collision cross sections for argon atoms](#)

A V Phelps, Chris H Greene, J P Burke Jr et al.

[CP violation, UK Phenomenology Workshop 2000](#)

Tobias Hurth, Choong Sun Kim, Claire Shepherd-Themistocleous et al.

[Elemental thin film depth profiles by ion beam analysis using simulated annealing - a new tool](#)

C Jeynes, N P Barradas, P K Marriott et al.

# Rutherford simple and multiple scattering by computer simulation

J M Paniagua<sup>1</sup>, J M Sánchez, J Moreno<sup>2</sup>, A Jiménez<sup>1</sup> and M Rufo<sup>1</sup>

<sup>1</sup> Departamento de Física, Escuela Politécnica, Avda. de la Universidad s/n, 10071 Cáceres, Spain

<sup>2</sup> Departamento de Informática, Escuela Politécnica, Avda. de la Universidad s/n, 10071 Cáceres, Spain

Received 2 May 2000, in final form 3 January 2001

## Abstract

This work presents, by means of a model of stochastic simulation, computer simulation of the experiments conducted by Geiger and Mardsen in which sheets of gold were bombarded by  $\alpha$ -particles, and which led to the production of the first nuclear atomic model. With them, the dependence of the cross section for Rutherford scattering on energy and atomic number of the incident particle and on the atomic number, composition and thickness of the target can be analysed. In addition, it is possible to identify the intervals in the angular distribution where single and multiple scattering predominates. Statistical summaries for the angular distributions obtained can also be analysed in terms of the variables mentioned above. The computer application has been produced with pedagogical use in mind for first year university students.

## 1. Introduction

The experiments conducted by Geiger and Mardsen in Rutherford's Laboratory on scattering  $\alpha$ -particles in the years 1911–1913 led to the discovery of the existence of the atomic nucleus and served to produce an atomic model that, although primitive at the time, formed the basis for the development of atomic and nuclear physics.

In these experiments, the investigators bombarded a sheet of gold, with a thickness of less than a micrometre, with  $\alpha$ -particles which came from the disintegration of radium and whose energy was about 5 MeV. They observed how most of them followed a straight line or were deflected from the initial path with small angles of deflection after passing through the target; however, surprisingly some of the particles were scattered through large angles, which was contrary to predictions based on Thomson's atomic model. Rutherford concluded that the large deflections did not come from the accumulated effect of scattering through a multitude of small angles, as would be expected according to Thomson's model, but rather from a single interaction between an incident particle and the atom. Therefore, he concluded that the atom must have a very intense electrical field located within it; a conclusion which led to the first nuclear atomic model.

The mathematical analysis of this experiment led to the derivation of an equation for the cross section by Rutherford scattering—and in general, by scattering due to forces inversely

proportional to the square of the distance between the interacting particles—which is consistent with the experimental results. This formulation is dealt with in several text books used by students who are studying scientific degrees, not only in the area of atomic physics [1], but also related to fields such as classical electrodynamics [2] and the dynamics of particles and systems [3], among others.

The execution of experiments that complement the theoretical aspects related to Rutherford scattering is undoubtedly a valuable didactic resource for students that take physics courses in the scientific field; however, the high cost of the necessary equipment (source of alpha particles, gold foil, fluorescent sheet, microscope, etc) and the risk that exposure to the ionizing radiation involves make experiments such as this one quite rare.

We have therefore designed a computer application that allows one to simulate the experiments conducted by Geiger and Mardsen, which allows diverse aspects of Rutherford scattering to be studied. Among them are: (a) the analysis of the dependency of the cross section on the angle of deflection, the energy of the incident particle and atomic number, both of the incident particle and of the target; (b) the study of the angular distribution produced by targets formed by a mixture of two types of atoms in proportions determined by the student; and (c) the analysis of the angular distribution according to the thickness of the target, which allows one to distinguish between the areas in which single scattering and multiple scattering predominate.

The application, developed using the Borlan Pascal Delphi 3.0 Compiler, works under Windows 9x and possesses great versatility when planning several experiments by means of the selection of parameters such as: the type and number of particles in the incident beam and their energy; the material (or materials) that form the target; the proportion in which they are mixed and the thickness of the foil. As output, the application gives us the number of impacts per angular interval of  $1^\circ$  width from  $0^\circ$  to  $180^\circ$  and the following statistical summaries: minimum and maximum angles, mean, standard deviation, square root of the mean squared scattering angle (RMS), median, and upper and lower quartiles. The maximum number of particles that can be pre-selected for the incident beam is  $10^6$  and the maximum thickness of the target is  $1 \mu\text{m}$ . The execution time of an experience with these characteristics takes approximately 120 h using a PC computer with a 450 MHz Pentium III processor. The application can be found on the web site <http://webepcc.unex.es/~ppmoreno>.

## 2. Description of the simulation model

The simulation model is based on an electrostatic interaction, which takes into consideration only the non-screened point Coulomb field and performs a classical treatment of the interaction. Therefore, this model will be valid to simulate experiments in which the energy of the incident particle is not large enough to involve the nuclear force.

The classical treatment is justified by the peculiarity of forces proportional to  $1/r^2$ , in which the exact quantum result does not contain the  $\hbar$  factor and therefore does not change when passing the classical limit. A simple calculation also leads to the supposition of fixed trajectories, considered by classical mechanics, and does not produce large errors in the cross section for Rutherford scattering. If  $\Delta b$  and  $\Delta p$  are the uncertainties in the impact parameter and momentum transferred by the incident particle, respectively, the classical treatment would only make sense if  $\Delta b \ll b$  and if  $\Delta p \ll p$ , since  $b\Delta p \gg \Delta b\Delta p \gg \hbar$  and therefore  $b\Delta p/\hbar \gg 1$ . For example, for two extreme cases with scattering angles of  $90^\circ$  and of  $1^\circ$ , when 8 MeV  $\alpha$ -particles collide with a gold target,  $b\Delta p/\hbar$  takes the values of 14 and 32, respectively, which justifies the classical treatment of the problem [4].

Once the experiment is designed, the program simulates a cylindrical and homogeneous beam of particles that directs itself towards the atoms of the target. They are dispersed by the Coulomb interaction and registered by hypothetical ring-shaped detectors that cover the  $0$ – $180^\circ$  range with angular intervals of  $1^\circ$ . In order to simulate each particle of the beam, two random numbers (using the Borlan Pascal Delphi 3.0 random numbers generator),  $x$  and

$y$  are generated, which are constant in the interval  $(0, D_{\text{at}}/2)$ , where  $D_{\text{at}} = (\rho N_A/A)^{-1/3}$  is the inter-atomic distance ( $\rho =$  density,  $A =$  atomic mass of the target and  $N_A =$  Avogadro's number) [5]. These random numbers represent the position of the particle in relation to the longitudinal axis of the beam, where the impact parameter  $b$  is calculated from  $x$  and  $y$ , using the equation  $b = (x^2 + y^2)^{1/2}$ .

The mathematical description of the collisions between free particles is simplified considerably when a system of coordinates is taken, whose origin is at rest in relation to the centre of mass of the system. In this system, the projectile–target set is replaced by a single particle of mass  $\mu$  moving in a central force field, defined by the potential energy function  $U(r)$ . Since this function depends only on the distance of the particle from the scattering centre, and not on the orientation, the system possesses spheric symmetry and a rotation around the axis that passes through the scattering center, does not affect the equations of motion, therefore conserving the angular momentum of the system. The total energy (kinetic plus potential) of the system is expressed in polar coordinates  $(r, \theta)$  as

$$E = \frac{1}{2}\mu(\dot{r}^2 + r\dot{\theta}^2) + U(r). \quad (1)$$

From here, applying the conservation of energy and angular momentum laws to the projectile–target system, the deflection angle  $\theta$  is obtained [3] and is given by

$$\theta = \pi - 2 \cos^{-1} \frac{k/2T_0b}{\sqrt{1 + (k^2/(2T_0b)^2)}} \quad (2)$$

where  $k = q_p q_b / 4\pi \epsilon_0$  ( $q_p$  and  $q_b$  are the charges of the projectile and target, respectively),  $T_0$  is the energy of the incident particle,  $b$  is the impact parameter and  $\epsilon_0$  is the permittivity of empty space.

Since the real measurements are carried out in the laboratory coordinates (L coordinates), we had to transform this result, which was valid only for the centre-of-mass coordinates (C coordinates). A derivation of the equation that relates the deflection angle in the L coordinates,  $\tau$ , to that of the centre of mass,  $\theta$ , can be found in Marion's book [3] and is given by

$$\tau = \tan^{-1} \frac{\sin \theta}{\cos \theta + (m_p/m_b)} \quad (3)$$

where  $m_p$  and  $m_b$  are the masses of the projectile and the target, respectively.

Normally, the mass of the projectile is much less than that of the target, which makes  $\tau \approx \theta$ , and furthermore the loss of energy suffered by the projectile in the collision is very small. However, when the masses of the projectile and of the target are not very different, or if the projectile suffers many collisions, the loss of energy can be considerable. This loss of energy is expressed by means of the following relationship between the masses of the projectile and target and angle of deflection [3]:

$$\Delta E = \frac{2m_p m_b}{(m_p + m_b)^2} (1 - \cos \theta). \quad (4)$$

These expressions have been deduced assuming that each projectile suffers only one interaction. Normally, the targets have such a thickness that when a projectile passes through them it suffers various deflections. In order to obtain the final angle after several collisions, we have used a Cartesian system of  $XYZ$  axes and assumed that the initial beam is oriented along the  $Z$ -axis. This direction would be characterized, therefore, by the unit vector  $(0, 0, 1)$ . If the random numbers through which we have obtained the impact parameter are  $x$  and  $y$ , the final direction of the particle can be obtained through two rotations: one around the  $Z$ -axis making a clockwise rotation  $\alpha = \tan^{-1}(x/y)$ , and another around the new  $X$ -axis, making a clockwise rotation  $\tau$  (equation (3)), so that the  $Z$ -axis is made to coincide with the direction of the scattered particle (see figure 1).

Therefore, the first rotation may be obtained by applying the matrix

$$\begin{pmatrix} \cos \alpha & \sin \alpha & 0 \\ -\sin \alpha & \cos \alpha & 0 \\ 0 & 0 & 1 \end{pmatrix}$$

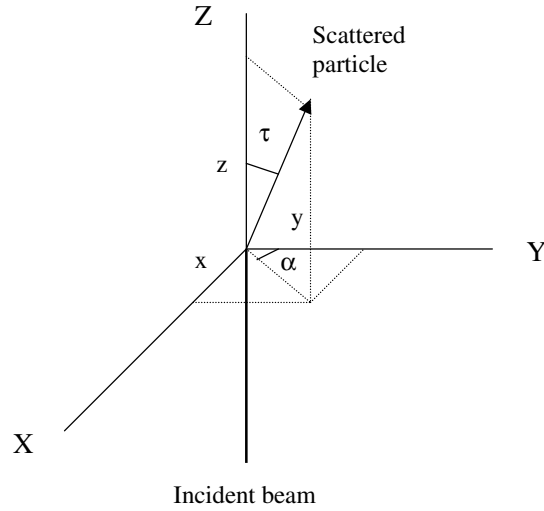


**Figure 1.** The relationship of the direction of the scattered particle to the direction of the incident particle through the angles  $\tau$  and  $\alpha$ .

to the vector that represents the incident particle, and the  $\tau$  rotation by applying the matrix

$$\begin{pmatrix} 1 & 0 & 0 \\ 0 & \cos \tau & -\sin \tau \\ 0 & \sin \tau & \cos \tau \end{pmatrix}$$

to the vector that is the result of the first rotation. The direction of the particle after this collision will be obtained from the matrix equation

$$\begin{pmatrix} x_1 \\ y_1 \\ z_1 \end{pmatrix} = \begin{pmatrix} 1 & 0 & 0 \\ 0 & \cos \tau & -\sin \tau \\ 0 & \sin \tau & \cos \tau \end{pmatrix} \begin{pmatrix} \cos \alpha & \sin \alpha & 0 \\ -\sin \alpha & \cos \alpha & 0 \\ 0 & 0 & 1 \end{pmatrix} \begin{pmatrix} x_0 \\ y_0 \\ z_0 \end{pmatrix} \quad (5)$$

where  $x_1$ ,  $y_1$  and  $z_1$  represent the coordinates of the vector after the first collision and  $x_0$ ,  $y_0$  and  $z_0$  are those of the vector that represent the direction of the particle before suffering the collision.

Supposing that the initial direction is  $(0, 0, 1)$  and applying equation (5) as many times as the particle suffers a collision, the direction of the emergent particle will be obtained, and will be characterized by the vector  $\mathbf{r} = (x_n, y_n, z_n)$ . Starting from here, we obtain the  $\alpha$  and  $\tau$  angles. The first one is obtained from the  $x_n$  and  $y_n$  coordinates of the  $\mathbf{r}$  vector by means of the  $\alpha = \tan^{-1}(x_n/y_n)$  equation, and  $\tau$  is obtained from the  $\mathbf{r} \cdot \mathbf{k}$  dot product, where  $\mathbf{k}$  is the unit vector in the direction of the  $Z$ -axis. Since  $\mathbf{r} \cdot \mathbf{k} = r \cos \tau$ , we have that  $\cos \tau = \mathbf{r} \cdot \mathbf{k}/r$ , and therefore

$$\tau = \cos^{-1} \frac{z_n}{\sqrt{x_n^2 + y_n^2 + z_n^2}}. \quad (6)$$

### 3. Single scattering

The scattering angles  $\theta$  and  $\tau$  in the C and L coordinates are related through equation (3). From this equation, it is deduced that if the mass of the projectile is very much less than that of the target, both angles are practically equal, as are the scattering cross sections. Given that in our simulation the detectors are rings that register all of the events between the angles  $\tau$  and

**Table 1.** The mean number of scattered particles in different angular intervals, the standard deviation (SD) and the coefficient of variation (CV) obtained when conducting 10 experiments in which beams of  $10^6$   $\alpha$ -particles with energy 0.5 MeV strike gold targets.

Interval	Mean	SD	CV (%)
1–2°	23 081	107	0.46
2–3°	4264	76	1.8
3–4°	1495	20	1.3
4–5°	380	20	5.3
5–6°	222	15	6.8
6–7°	143	8	5.6
7–8°	101	9	8.9
8–9°	74	6	8.1
9–10°	57	8	14.0
10–11°	40	6	15.0

$\tau + d\tau$ , in order to compare the results obtained with the cross section by Rutherford scattering  $d\sigma$ , per unit of solid  $d\Omega$  angle [1],

$$\frac{d\sigma}{d\Omega} = \frac{z^2 Z^2 e^4}{256\pi^2 \varepsilon_0^2 E^2 \sin^4(\tau/2)} \quad (7)$$

(where  $z$  and  $Z$  are the atomic numbers of the projectile and of the target, respectively, and  $E$  is the energy of the projectile), the number of impacts of each angular interval have been divided by  $d\Omega = 2\pi \sin \tau d\tau$ .

In the experiments that are presented in this section, only targets with a thickness such that each particle of the incident beam suffers only one collision have been considered.

### 3.1. Variability of the results

Given that a random number generator is used in the simulation, if the same experiment is repeated many times, the statistical summaries will be different in each one of them. In order to analyse the range of variation of the statistical summaries (number of particles scattered in each angular interval, mean, median, RMS angle  $(\langle \tau \rangle^{1/2})$ , standard deviation and interquartile range), an experiment has been repeated ten times, in which a  $10^6$   $\alpha$ -particle beam with energy 0.5 MeV interacts with a gold target. In table 1, the number of deflections detected in the different angular intervals is shown, as well as the standard deviation and the coefficient of variation. It can be seen that the number of particles scattered through different angular intervals decreases when the angle increases. The standard deviation also decreases and this decrease is proportional to the square root of the number of particles detected in each angular interval, as is expected when considering a simulated phenomenon by means of the generation of uniform random numbers. The coefficient of variation, which indicates the relative dispersion of the results, increases when the number of events decreases, in our case making it from 0.46% in the 1–2° angular interval to 15% in the 10–11° interval, which allows us to estimate the error made when characterizing the angular distribution through a single experiment.

The average values of the statistical summaries obtained in the ten experiments remain very stable up to the second decimal place. More precisely, values of 0.35°, 0.25° and 0.64° have been obtained for the mean, median and  $\langle \tau \rangle^{1/2}$ , all of them with a coefficient of variation smaller than 3%, while the dispersion parameters obtained were 0.53° and 0.15° for the standard deviation and the interquartile range, respectively, both with a coefficient of variation of smaller than 4%.

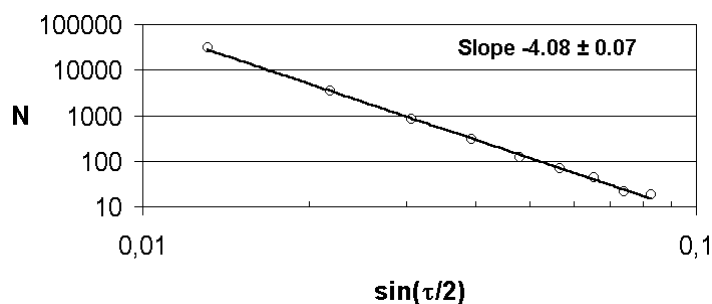


**Figure 2.** A log–log representation of the number of scattered particles  $N$  versus  $\sin(\tau/2)$ . (Beam,  $2 \times 10^7$   $\alpha$ -particles; energy, 5 MeV; target, Au).

### 3.2. Angular distribution

One of the typical experiments that we can conduct with this simulation model consists of a beam of  $\alpha$ -particles striking a gold sheet and the analysis of the angular distribution obtained. Given that the number of scattered particles decreases greatly when the deflection angle increases, with the objective of obtaining good statistical parameters, we conducted an experiment 20 times in which a beam of  $10^6$   $\alpha$ -particles with energy 5 MeV struck a gold target, which is equivalent to having a beam of  $2 \times 10^7$  particles. Figure 2 shows the number of events per unit of solid angle versus  $\sin(\tau/2)$ . In this figure, it can be observed that the number of events decreases when the angle increases, distributing the points in a straight line with a slope of  $-4.08 \pm 0.07$  (standard deviation) when a log–log representation is executed. This result indicates the existence of a power-law relationship between both variables such as the one that predicts the cross section by Rutherford scattering from equation (7).

### 3.3. Cross section versus energy and atomic number of the projectile

The variation of the cross section by Rutherford scattering with the energy of the projectile can be proven with the execution of adequate experiments. For this reason, we have simulated experiments in which  $\alpha$ -particle beams with energy between 1 and 8 MeV strike gold and uranium targets. Figure 3 shows the events that occurred in the  $1$ – $2^\circ$  angular interval in these experiments in a log–log scale, versus the energy of the particles. As can be observed, there is a power-law dependence among both variables, where the slope is  $-1.978 \pm 0.023$  in the case of gold and  $-2.00 \pm 0.02$  in the case of uranium. These results indicate that the cross section decreases according to the inverse of the square of the energy of the incident particles, as equation (7) predicts. From the analysis of statistical data for the angular distributions obtained in these experiments, we find out that the mean, median,  $\langle \tau \rangle^{1/2}$ , standard deviation and interquartile range increase linearly with the inverse of the energy of the incident particles. When a linear correlation analysis is performed, significant correlation coefficients larger than 0.99 are obtained.

The variation of the cross section with the atomic number of the projectile has been analysed by means of the simulation of experiments in which we have used protons,  $\alpha$ -particles, nuclei of lithium, beryllium, boron and carbon, and as a target, sheets of gold. From the analysis of the results of these experiments, we have noticed that the number of deflections that occurred in each angular interval increases with the square of the atomic number of the projectile, as can be deduced from expression (7). In particular, when plotting linear regressions of the logarithm of the number of scattered particles in the  $1$ – $2^\circ$ ,  $2$ – $3^\circ$  and  $3$ – $4^\circ$  angular intervals versus the logarithm of the atomic number of the projectile, we obtain equations of straight lines with slopes of  $1.941 \pm 0.006$ ,  $1.9210 \pm 0.0008$  and  $2.012 \pm 0.023$ , respectively, all with correlation coefficients larger than 0.99. We have also performed linear correlation analysis

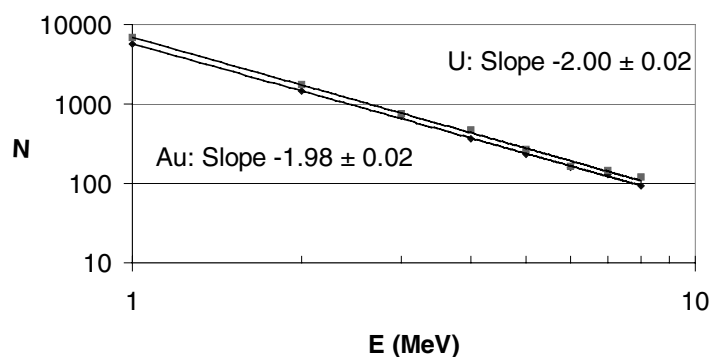


**Figure 3.** The number of scattered particles in the angular interval ( $1-2^\circ$ ),  $N$ , versus the energy of the projectile,  $E$ , for gold and uranium targets. (Beams of  $10^6$  particles with energies of between 1 and 8 MeV).

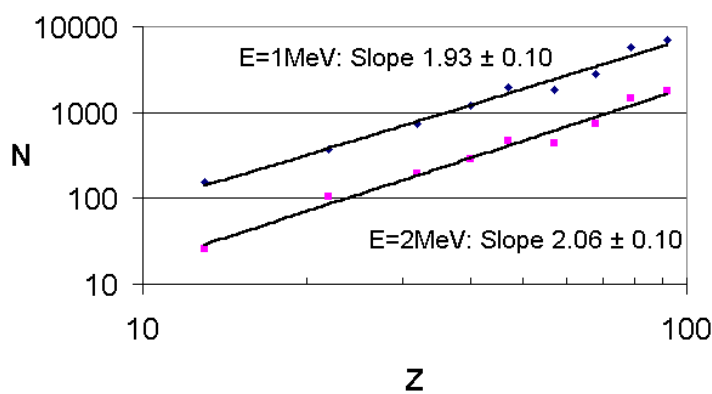


**Figure 4.** The number of scattered particles in the angular interval ( $1-2^\circ$ ),  $N$ , versus the atomic number of the target,  $Z$ , using beams of  $10^6$   $\alpha$ -particles with energies of 1 and 2 MeV.

of the mean, median,  $\langle \tau \rangle^{1/2}$  and the dispersion parameters versus the atomic number of the projectile obtaining significant correlation coefficients larger than 0.99.

#### 3.4. Cross section versus atomic number and composition of the target

In order to analyse the variation of the cross section with the atomic number of the target, we have conducted experiments in which we simulate beams of  $10^6$   $\alpha$ -particles of 1 and 2 MeV striking targets made of aluminium, titanium, germanium, zirconium, silver, lanthanum, erbium, gold and uranium. In figure 4, the number of counts that occurred in the  $1-2^\circ$  angular interval versus the atomic number of the target in these experiments is shown on a log-log scale. From this figure, it can be observed that the events increase linearly with the atomic number of the target, with slopes of  $1.93 \pm 0.10$  when the energy is 1 MeV, and  $2.06 \pm 0.10$  when the energy is 2 MeV, as equation (7) predicts. From the statistical analysis of the characteristic parameters of the angular distribution, we deduce that the mean, median,  $\langle \tau \rangle^{1/2}$  and the dispersion parameters increase linearly with the atomic number of the target.

The computer application allows us to design experiments in which the beams of particles irradiate targets made of two different types of atoms in proportions that the student may select. For example, we have carried out experiments consisting of beams of  $\alpha$ -particles with energy 0.5 MeV and targets made of gold and silver with the following proportions of gold: 0, 10, 20,



30, 40, 50, 60, 70, 80, 90 and 100%, and the rest of silver. We have noticed that the number of scattered particles in the different angular intervals increases linearly when the proportion of gold increases (this is a logical result, since gold possesses the largest atomic number of the two elements that form the target). For example, in the  $1-2^\circ$  interval, the slope and intercept obtained are  $153 \pm 2$  and  $8100 \pm 100$ , respectively, which indicates that for each 1% of gold in the target the number of deflected particles in this interval increases by  $153 \pm 2$  over the  $8100 \pm 100$  value that would correspond to the target made exclusively of silver. Therefore, in a hypothetical target made of gold and silver in unknown proportions, the composition could be checked by conducting experiments such as the one described and applying the equation  $Y = aX + b$ , where  $Y$  is the number of scattered particles in the angular interval ( $1-2^\circ$ ) and  $X$  is the percentage of gold. Therefore,  $X = (Y - b)/a$ , the relative error  $\delta X/X$  is

$$\frac{\delta X}{X} = \frac{\delta Y + \delta b}{Y - b} + \frac{\delta a}{a} \quad (8)$$

and the uncertainty in the determination of the percentage of gold is

$$\delta X = \frac{\delta Y + \delta b}{a} + \frac{\delta a}{Y - b} X^2. \quad (9)$$

From this equation, we deduce that the smallest error would be obtained when the target was composed exclusively of silver, since in this case  $X = 0$  and  $\delta Y$  would be minimum; in contrast, the largest error would be obtained when  $X = 100\%$ , since in this case both  $X$  and  $\delta Y$  would be maximum. In particular, taking as absolute errors 1.96 times the standard deviation, to have 95% confidence level, we obtain absolute errors in the determination of the percentage of gold present in the target, in the two previous extreme cases, of 2.4% and 5.9%, respectively. These results offer interesting information about the precision that can be obtained in the determination of the different proportions of the elements present in the target when experiments like the ones described in this section are carried out.

#### 4. Multiple scattering

Up until now, we have considered the thickness of the target to be such that only one deflection per particle of the incident beam occurred. When the thickness increases, so does the number of deflections that each particle suffers. A particle that goes through matter of fine thickness will suffer many deviations of small angles and, generally, will emerge with a small angle, as a result of the statistical superimposition of a large number of deviations. Only on a very few occasions will the particle in a large angle divert substantially, and since these events occur very rarely, this particle would have executed only one collision that will create a large deflection angle. The angular distribution can then be divided in two regions, one of comparatively large angles which only contains simple deflections and another one of very small angles corresponding to multiple scattering.

The most important quantity in the multiple scattering region, in which there is a large number of small deviations symmetrically distributed around the incident direction, is the RMS angle corresponding to a single deviation. This angle is defined by [2]

$$\langle \tau^2 \rangle = \frac{\int \tau^2 (d\sigma/d\Omega) d\Omega}{\int (d\sigma/d\Omega) d\Omega} \quad (10)$$

where  $d\sigma$  is the differential cross section and  $d\Omega$  is the differential solid angle. Since the collisions are independent events, by using the theorem of the central limit, it can be demonstrated that in a large number of collisions the angular distribution will approximately be a Gaussian around the direction of the incident beam with an average squared angle  $\langle T^2 \rangle = n \langle \tau^2 \rangle$  [2]. The mean squared angle is therefore proportional to the number of collisions

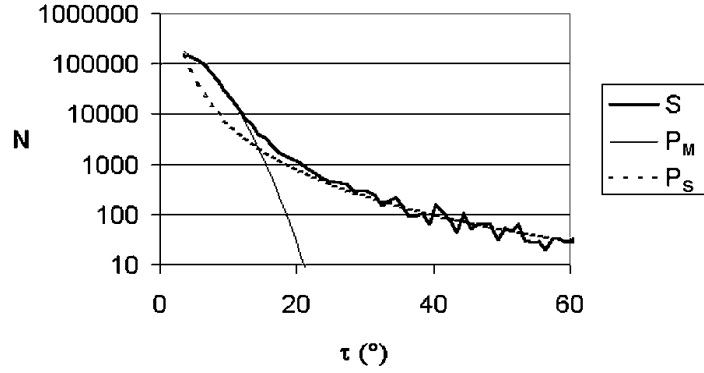


**Figure 5.** The angular distribution obtained when a beam of  $10^6$   $\alpha$ -particles with energy 5 MeV irradiates a  $1 \mu\text{m}$  thick gold target ( $S$ ). The theoretical distributions corresponding to single scattering given by equation (12),  $P_S$ , and multiple scattering given by equation (11),  $P_M$ , are also represented.

and to the thickness of the target. The resulting angular distribution in this region has a Gaussian shape, given by the expression [6]

$$P_M(\tau) d\tau \approx \frac{1}{\pi \langle \tau^2 \rangle} \exp\left(-\frac{\tau^2}{\langle \tau^2 \rangle}\right) d\tau. \quad (11)$$

In the area where simple scattering dominates, the angular distribution comes from the expression (7) that leads to a probability distribution characterized by the expression

$$P_S(\tau) d\tau \approx \frac{z^2 Z^2 e^4}{64\pi \epsilon_0^2 E^2 \sin^3(\tau/2)} d\tau. \quad (12)$$

In order to analyse the angular distribution produced when the particles of the incident beam suffer multiple deflections, we have simulated an experiment consisting of a beam of  $10^6$   $\alpha$ -particles with energy 5 MeV striking a  $1 \mu\text{m}$  thick gold target. This distribution is shown in figure 5, together with the theoretical distributions for multiple scattering  $P_M$ , given by equation (11), and simple scattering  $P_S$ , given by equation (12). It can be observed in figure 5 that the angular distribution obtained conforms well to the Gaussian distribution (11) in the angular interval ( $4$ – $12^\circ$ ); for larger angles, the Gaussian distribution decreases rapidly and does not reproduce the values obtained in the simulation, since we come into the area in which simple scattering begins to be important. The theoretical angular distribution by simple scattering given by equation (12) conforms well to the data obtained in the simulation for angles in excess of  $24^\circ$ ; for values smaller than this angle, the number of deflections obtained in each angular interval is greater than that given by equation (12) since multiple scattering acquires importance there. The angular interval between  $12^\circ$  and  $24^\circ$  corresponds to the transition between simple and multiple scattering.

We have also analysed the way in which the statistical summaries vary when the thickness of the target varies. To carry out this analysis, we have executed a number of experiments in which beams of  $10^6$   $\alpha$ -particles of energy 5 MeV irradiate gold targets with thicknesses between 1 nm and  $1 \mu\text{m}$  and whose results are shown in table 2. From this table it can be observed how the mean, median and  $\langle \tau \rangle^{1/2}$  increase when the thickness of the target does too, although not in a linear way. When the logarithm of these parameters is plotted against the logarithm of thickness of the target, we obtained straight lines with a slope of  $0.549 \pm 0.003$  for the mean,  $0.570 \pm 0.004$  for the median and  $0.494 \pm 0.002$  for the RMS angle, which indicates that these parameters vary, approximately, with the square root of the thickness of the target. This result, as far as the RMS angle, is logical if we take notice of the  $\langle T^2 \rangle = n \langle \tau^2 \rangle$  relationship

**Table 2.** Statistical data of the angular distributions obtained in the simulation of the interactions of beams of  $10^6$   $\alpha$ -particles with energy 0.5 MeV over targets of Au of different thicknesses ( $q$ , lower quartile,  $Q$ , upper quartile; SD, standard deviation;  $\langle\tau\rangle^{1/2}$ , RMS angle). In the last row, the number of scattered particles for angles greater than  $90^\circ$  are shown.

	Thickness ( $\mu\text{m}$ )						
	0.001	0.01	0.05	0.1	0.4	0.7	1
Minimum	0.00	0.00	0.00	0.00	0.00	0.01	0.01
$q$	0.06	0.19	0.51	0.77	1.69	2.33	2.84
Median	0.09	0.31	0.81	1.22	2.68	3.67	4.49
$Q$	0.14	0.48	1.21	1.80	3.93	5.38	6.56
Maximum	48.13	70.02	120.1	123.61	124.56	123.90	124.00
Mean	0.12	0.40	0.99	1.47	3.15	4.28	5.20
SD	0.18	0.53	1.09	1.50	2.75	3.49	4.11
$\langle\tau^2\rangle^{1/2}$	0.22	0.66	1.47	2.09	4.18	5.52	6.63
$N > 90^\circ$	0	0	8	16	47	76	126

previously cited. Another effect that occurs when the thickness of the target increases, as a consequence of the increased number of deflections which each incident beam particle suffers, is that the probability that a large scattering angle occurs increases. The last row of table 2 shows the number of particles that come out of the target with deflections greater than  $90^\circ$ . It can be observed in this table that for thicknesses of 0.001 and 0.01  $\mu\text{m}$  none exist; for 0.05  $\mu\text{m}$  there are eight particles, and from there on the number increases approximately linearly with thickness. It is interesting to emphasize that, for a target thickness of 0.4  $\mu\text{m}$ , the number of particles that come out with a scattering angle greater than  $90^\circ$  is 47, out of  $10^6$  particles that formed the beam, which is equivalent to 0.94 deflections greater than  $90^\circ$  per each 20 000 particles that strike the target. This result is equivalent to that obtained by Geiger and Mardsen, in which approximately 1 particle out of 20 000 was scattered with angles greater than  $90^\circ$  [1] when using a 0.4  $\mu\text{m}$  thick gold target and  $\alpha$ -particles from a source of radium, whose approximate energy is 5 MeV [1].

## 5. Conclusions

We have designed a computer program that simulates the experiment conducted by Geiger and Mardsen in 1911, which was the first step that led to the actual theory of the atom. The application is designed to be used as a laboratory experiment simulated by a computer for first year university students who take classes such as atomic physics, classical electrodynamics and dynamics of particles and systems.

The experiments that can be conducted, and that have also served to validate the simulation model, can be used by students to:

- check the results statistically, considering the number of dispersions that occur in each angular interval and the average, median,  $\langle\tau\rangle^{1/2}$ , standard deviation and interquartile range of the angles;
- check the dependence of the cross section by Coulomb dispersion with  $\sin^4(\tau/2)$ ;
- study the influence of energy ( $E$ ) and the atomic number of the projectile ( $Z_P$ ) in the angular distribution and statistical summaries; the numbers of scattered particles in each angular interval vary according to  $1/E^2$  and  $Z_P^2$ , and the statistical summaries average, median,  $\langle\tau\rangle^{1/2}$ , standard deviation and interquartile range vary according to  $1/E$  and  $Z_P$ ;
- observe the dependence of the above variables on the atomic number of the target ( $Z_B$ ); the cross section by Coulomb dispersion varies according to  $Z_B^2$ , and the statistical summaries vary according to  $Z_B$ ;

- analyse the angular distributions caused by targets made of two different atoms and find out, by performing several experiments, the percentage of each atom that composes the target and its error;
- identify the area where single and multiple scattering predominate in the angular distribution, obtained using a beam of particles striking a target of great thickness;
- check that the statistical summaries increase with the square root of the target thickness.

## References

- [1] Enge H A, Wehr M R and Richards J A 1979 *Introduction to Atomic Physics* (New York: Addison-Wesley)
- [2] Jackson J D 1975 *Classical Electrodynamics* (New York: Wiley)
- [3] Marion J B 1975 *Classical Dynamics of Particles and Systems* (New York: Academic)
- [4] Krane K S 1988 *Introductory Nuclear Physics* (New York: Wiley)
- [5] French A P 1982 *Introducción a la Física Cuántica* (Barcelona: Reverté)
- [6] Leo W 1992 *Techniques for Nuclear and Particle Physics Experiments* (Berlin: Springer)